Am J Physiol Renal Physiol 297: F1575–F1586, 2009.
First published September 23, 2009; doi:10.1152/ajprenal.90762.2008.

Angiotensin II and hypertonicity modulate proximal tubular aquaporin 1 expression

Richard Bouley,[1] Zaira Palomino,[2] Shiow-Shih Tang,[3] Paula Nunes,[1] Hiroyuki Kobori,[4] Hua A. Lu,[1] Winnie W. Shum,[1] Ivan Sabolic,[5] Dennis Brown,[1] Julie R. Ingelfinger,[6] and Flavia F. Jung[4,7]

[1]*Massachusetts General Hospital Center for Systems Biology, Program in Membrane Biology and Nephrology Division, Massachusetts General Hospital, and Harvard Medical School, Boston, Massachusetts;* [2]*Disciplina de Nephrologia da Escola Paulista de Medicina, Universidade Federal de São Paulo, Sao Paulo, Brazil;* [3]*Medicine and Cardiology, Brigham and Women's Hospital, Harvard Medical School, Boston, Massachusetts;* [4]*Department of Physiology and Hypertension, Tulane University Health Sciences Center, New Orleans, Louisiana;* [5]*Molecular Toxicology, Institute for Medical Research and Occupational Health, Zagreb, Croatia;* [6]*Pediatric Nephrology, Massachusetts General Hospital, and Harvard Medical School, Boston, Massachusetts; and* [7]*Department of Pediatrics, Georgetown University, Washington, District of Columbia*

Submitted 23 December 2008; accepted in final form 20 September 2009

Bouley R, Palomino Z, Tang S-S, Nunes P, Kobori H, Lu HA, Shum WW, Sabolic I, Brown D, Ingelfinger JR, Jung FF. Angiotensin II and hypertonicity modulate proximal tubular aquaporin 1 expression. *Am J Physiol Renal Physiol* 297: F1575–F1586, 2009. First published September 23, 2009; doi:10.1152/ajprenal.90762.2008.—Aquaporin 1 (AQP1) is the major water channel in the renal proximal tubule (PT) and thin descending limb of Henle, but its regulation remains elusive. Here, we investigated the effect of ANG II, a key mediator of body water homeostasis, on AQP1 expression in immortalized rat proximal tubule cells (IRPTC) and rat kidney. Real-time PCR on IRPTC exposed to ANG II for 12 h revealed a biphasic effect AQP1 mRNA increased dose dependently in response to 10^{-12} to 10^{-8} M ANG II but decreased by 50% with 10^{-7} M ANG II. The twofold increase of AQP1 mRNA in the presence of 10^{-8} M ANG II was abolished by the AT_1 receptor blocker losartan. Hypertonicity due to either NaCl or mannitol also upregulated AQP1 mRNA by three- and twofold, respectively. Immunocytochemistry and Western blotting revealed a two- to threefold increase in AQP1 protein expression in IRPTC exposed concomitantly to ANG II (10^{-8}M) and hypertonic medium (either NaCl or mannitol), indicating that these stimuli were not additive. Three-dimensional reconstruction of confocal images suggested that AQP1 expression was increased by ANG II in both the apical and basolateral poles of IRPTC. In vivo studies showed that short-term ANG II infusion had a diuretic effect, while this effect was attenuated after several days of ANG II infusion. After 10 days, we observed a twofold increase in AQP1 expression in the PT and thin descending limb of Henle of ANG II-infused rats that was abolished when rats were treated with the selective AT_1-receptor antagonist olmesartan. Thus ANG II increases AQP1 expression in vitro and in vivo via direct interaction with the AT_1 receptor, providing an important regulatory mechanism to link PT water reabsorption to body fluid homeostasis via the renin-angiotensin system.

renin angiotensin system; proximal tubule

ANG II, the major effector of the renin-angiotensin system (RAS) (37), plays direct and indirect roles in water and salt homeostasis. In addition to its regulation of renal blood flow, glomerular filtration, and aldosterone secretion, ANG II binding to ANG II type 1 receptors (AT_1R) located in kidney proximal tubules additionally modulates sodium and bicarbonate reabsorption (22). AT_1R is broadly distributed in the kidney vasculature and the proximal tubule, medullary thick ascending limb, and all segments of the collecting duct (45–47). Lee et al. (39) demonstrated that ANG II can potentiate aquaporin 2 (AQP2) membrane insertion in response to vasopressin and that this effect can be blocked by candesartan, an AT_1R blocker, in primary cultured rat inner medullary collecting duct cells. Furthermore, ANG II was also shown to downregulate the expression of the urea transporter UT-A1, as well as that of the vasopressin-sensitive water channel AQP2 (35) in the rat kidney. In addition, ANG II upregulates vasopressin receptor type 2 (V2R) expression in the rat (68). Thus ANG II appears to play an important role in water reabsorption via its direct and indirect actions on regulation of the vasopressin-sensitive water channel AQP2 and other components of the urinary concentrating mechanism. However, the relationship between ANG II and other water channels in the kidney, including AQP1, is not well established.

The lack of urine concentrating ability observed in AQP1 knockout mice (52, 57, 69) highlights the importance of this transmembrane water channel protein, which is present in plasma membranes of several transporting epithelia, including the luminal and basolateral domains of renal proximal tubule and thin descending limb of Henle (TDLH) cells (23, 51, 54). Together, these two nephron segments are responsible for reabsorbing 80% of the fluid from the glomerular filtrate (36). Most of the remaining 20% is reabsorbed by AQP2 water channels in the distal nephron and collecting ducts.

In contrast to AQP2, the potential mechanisms by which AQP1 is regulated in renal proximal tubule cells remain largely unexplored. It has been generally thought that the effects of ANG II on proximal tubule fluid transport are secondary to altered electrolyte transport. While hypertonic NaCl has been shown to upregulate AQP1 expression in cultured renal epithelial cells (31), a potential role for ANG II in modulation of the AQP1 water channel in proximal tubule cells has not been investigated. Wintour et al. (67) demonstrated an increase of AQP1 mRNA in the sheep fetal kidney after infusion of ANG I. Additionally, Imai et al. (27) demonstrated suppression of AQP1 in peritoneal membranes of Wistar-Kyoto rats following treatment with either an angiotensin converting enzyme (ACE) inhibitor or an AT_1R antagonist (ARB), suggesting that the RAS plays an important role in the regulation of water trans-

Address for reprint requests and other correspondence: R. Bouley, Center for Systems Biology, Program in Membrane Biology, Nephrology Division, Massachusetts General Hospital, Harvard Medical School, CPZN 8150, 185 Cambridge St., Boston, MA 02114 (e-mail: Bouley.Richard@mgh.harvard.edu).

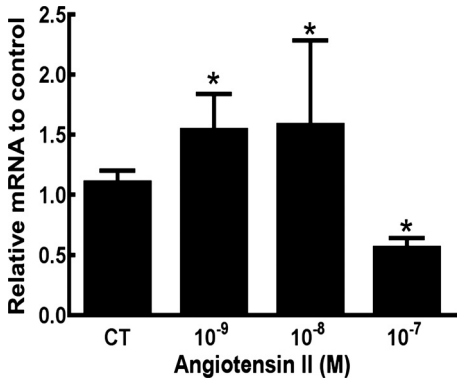

Fig. 1. Real-time PCR shows that ANG II has a biphasic effect on aquaporin 1 (AQP1) mRNA regulation. Immortalized rat proximal tubule cells (IRPTC) were incubated in the absence or presence of various concentrations of ANG II for 12 h, and AQP1 mRNA expression was assessed by real-time PCR. AQP1 mRNA levels are reported as values relative to the level of AQP1 mRNA in the absence of ANG II [control (CT)]. AQP1 mRNA level expression was upregulated in the presence of ANG II (10^{-8} and 10^{-9} M), while it is downregulated in the presence of a higher concentration of ANG II (10^{-7} M). Data are means ± SD; $n = 8$. *$P < 0.001$.

port in the peritoneum. Studies (5, 10, 20, 43, 59) using isolated perfused tubules or micropuncture have demonstrated substantial effects of ANG II on salt and water transport in the proximal tubule. Data from such studies (20, 32, 41, 56) suggest that not only is the RAS important in the regulation of hemodynamics but also in sodium reabsorption and tubuloglomerular feedback.

The present study aimed to examine the influence of ANG II on AQP1 expression in proximal tubule cells and to determine whether sodium chloride in the presence and absence of ANG II alters AQP1 expression. The effect of ANG II was studied in vitro using immortalized rat proximal tubule epithelial cells (IRPTC), which endogenously express AQP1 and all components of the RAS (61, 62) and in vivo using Sprague-Dawley rats. Our results indicate that both ANG II and hypertonicity modulate AQP1 mRNA and protein expression in a time- and dose-dependent manner in proximal tubules.

MATERIALS AND METHODS

Cell culture, reagents, and antibodies. All cell culture reagents were purchased from Invitrogen (Carlsbad, CA), and ANG II and inorganic salts were purchased from Sigma (St. Louis, MO). For this study, we used IRPTC to study the effect of the ANG II or NaCl exposure on AQP1 mRNA and protein expression (61, 62). The cell line was maintained in low glucose (5.5 mM), low sodium (81 mM) DMEM containing 25 mM HEPES. The cell culture medium was supplemented with 5% FCS, 100 U/ml penicillin, 100 μg/ml streptomycin, and 0.01 mM nonessential amino acids. In some experiments, as indicated below, NaCl was added to the low sodium medium to mimic normal serum content of 150 mM or to raise the NaCl concentration to 220 mM.

Before initiation of experiments, IRPTC were preincubated in serum-free medium (DMEM) containing 84 mM NaCl, and 0.5% BSA for 24 h. ANG II was then added, and cells were incubated for 1, 6, and 12 h at 37°C in the presence of 0, 10^{-12}, 10^{-9}, 10^{-8}, and 10^{-7} M ANG II. Losartan, an AT_1R blocker, and PD123319 (10 μM), an AT_2R blocker, were used as indicated below.

In addition, IRPTC were incubated in medium containing various concentrations of NaCl to study the effect of hypertonicity on AQP1 mRNA and AQP1 protein expression. Cells were incubated with low glucose, low sodium DMEM into which 90, 150, and 220 mM of NaCl had been added. Thus cells were exposed to normal (310 mosM), medium (415 mosM), and high osmolarity (550 mosM). To distinguish between the hyperosmotic and tonicity effects of NaCl, DMEM containing 440 mM of mannitol (740 mosM) was also used. The effects of combined exposure for 12 h at 37°C to hyperosmotic medium and ANG II (10^{-8} M) were also studied.

Animal treatment. Animal experiments were approved by the Massachusetts General Hospital Institutional Committee on Research Animal Care in accordance with the National Institutes of Health's *Guide for the Care and Use of Laboratory Animals*. Male Sprague-Dawley rats (Charles River Laboratories, Wilmington, MA) were housed for 24 h in metabolic cages immediately before treatment (*day 0*). The day of the experiment rats were anesthetized with isofluorane, and Alzet osmotic minipumps (Durect, Cupertino, CA) delivering either a solution of acetic acid 5% (sham) or ANG II diluted in acetic acid 5% solution (80 ng/min) were implanted subcutaneously on the back of the rats. A group of ANG II-treated rats received food containing a nonpeptidic ANG II antagonist (olmesartan, 5 mg/day) as previously described (37). Animals were again housed in metabolic cages and maintained in a temperature-controlled room regulated on a 12-h light-dark cycle with free access to the water. All animals were fed with ground pellets mixed or not mixed with olmesartan (Prolab IsoproRMH3000; LabDiet, Richmond, IN). Mean blood pressures were measured in conscious rats using tail-cuff plethysmography at *day 10* (CODA System; Kent Scientific, Torrington, CT). Urine and blood osmolarities were measured using an osmometer (Wescor, Logan, UT). At the termination of treatment, animals were euthanized, and one kidney was harvested for Western blot analysis, while the other was fixed for immunocytochemistry.

mRNA quantification by RT-PCR. IRPTC total RNA was isolated using TRIzol reagent (Invitrogen) according to the manufacturer's instructions. The RNA was treated with DNase I (Ambion, Austin, TX) to eliminate contamination by genomic DNA, and the final RNA concentration was standardized to 0.75 μg/μl. The integrity of the RNA was assessed by agarose gel electrophoresis. One-step real-time RT-PCR was carried out on a real-time thermal cycler (iCycler; Bio-Rad Life Sciences, Hercules, CA) using a QuantiTect SYBR Green RT-PCR kit (Qiagen, Valencia, CA). The method allows the reverse transcription and PCR to be carried out in a single step in the same reaction tube. The fluorescent dye SYBR Green I was included in the PCR master mix; in addition, the reaction was spiked with 0.5 μl of 1 μM fluorescein for background reference. The threshold cycle number (C_t) for RT-PCR was set by the cycler software.

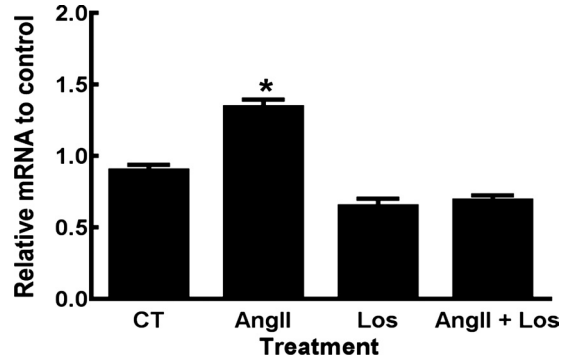

Fig. 2. Real-time PCR demonstrates that losartan (Los) inhibits the ANG II-induced increase in AQP1 mRNA . Real-time PCR analysis showed an increase in the level of AQP1 mRNA in IRPTC treated 12 h in the presence of ANG II (10^{-8} M) compared with the level of AQP1 mRNA in untreated cells (CT). This increase in AQP1 mRNA expression was abolished when ANG II-treated cells were also incubated in the presence of 10^{-5} M losartan (Los), a selective ANG II receptor type 1 antagonist. Losartan alone produced a significantly decreased of AQP1 mRNA level in IRPTC. Data are means ± SD; $n = 8$. *$P < 0.001$.

PCR primers (22–24 bp) for AQP1 (AQP1 sense: 5-GCT GTC ATG TAT ATC ATC GCC CAG-3; and AQP1 anti-sense: 5-AGG TCA TTT CGG CCA AGT GAG T-3) and GAPDH (GAPDH sense: 5-TGT TCC AGT ATG ACT CTA CCC ACG-3; and antisense: 5-GAA GAT GGT GAT TGG TTT CCC GTT-3) were designed using commercial software (Beacon Designer; Bio-Rad Life Sciences) to produce an amplicon length of 107 bp. Optimal primer concentration for PCR was determined separately for each primer pair. Each reaction was run in triplicate, and reaction tubes with target primers and those with GAPDH primers were always included in the same PCR run. To test primer efficiencies, the one-step RT-PCR was run with each target primer/GAPDH primer combination on an mRNA template dilution series up to a dilution factor of 1:100. The ΔC_t $\{C_t[\text{target}] - C_t[\text{GAPDH}]\}$ over the dilution range was constant for each primer pair, indicating equal primer efficiencies of the target and reference (GAPDH) primers, as required for the comparative C_t method (44) .

Relative quantification was achieved by the comparative $2^{-\Delta(\Delta Ct)}$ (44). The relative increase/decrease (fold-induction/repression) of mRNA of target × in the experimental group was calculated using the control group as the calibrator: $2^{-\Delta(\Delta Ct)}$, where $\Delta(\Delta Ct)$ is: $\{C_{t.x}[\text{AQP1}] - C_{t.\text{GAPDH}}[\text{AQP1}]\} - \{C_{t.x}[\text{control}] - C_{t.\text{GAPDH}}[\text{control}]\}$.

Immunocytochemistry. Immunocytochemistry studies were performed on 90% confluent cells grown on 12-mm coverslips. IRPTC

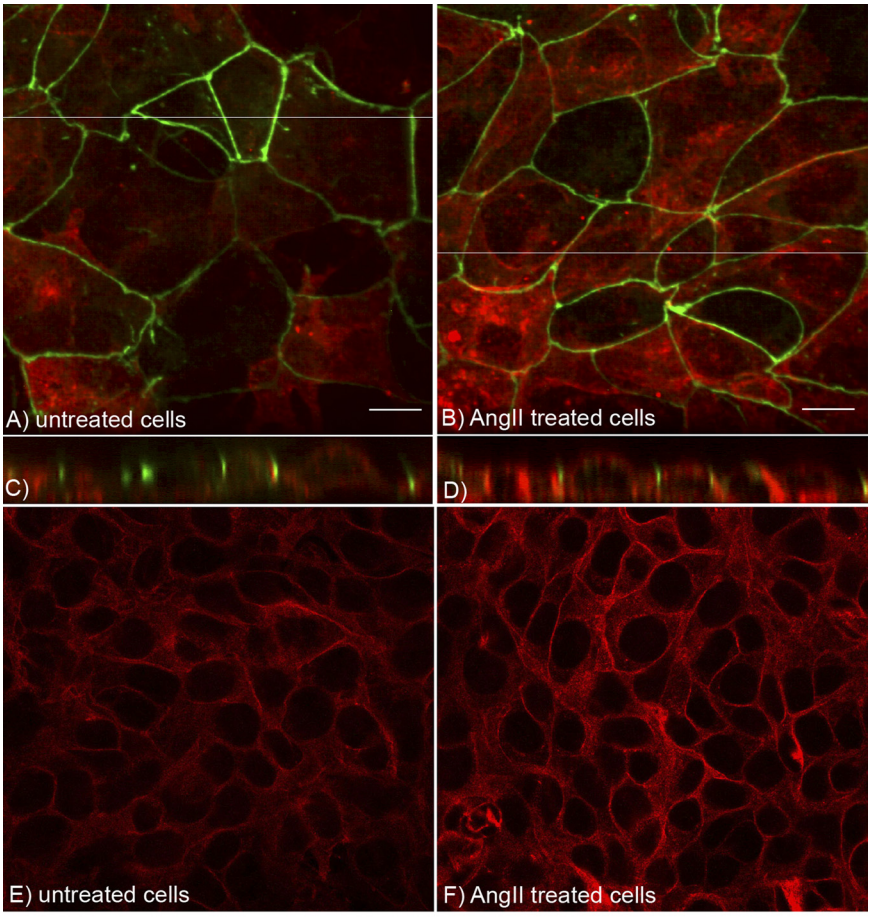

Fig. 3. Confocal microscopy reveals AQP1 increases both apically and basolaterally upon stimulation with ANG II (10^{-8} M). *A–D*: maximum projection and *XZ* slice (taken at the white line) of three-dimensional reconstructions of IRPTC incubated in the absence (*A* and *C*) or the presence of ANG II (10^{-8} M; *B* and *D*) for 12 h. The *Z* projections reveal an increase of AQP1 (red) staining on both apical regions [above the zonula occludens-1 (green) staining] as well as in basolateral membranes in the presence of ANG II. Staining intensity of AQP1 in a single midnuclear confocal plane is illustrated for untreated IRPTC (*E*) or cells treated with ANG II (*F*; 10^{-8} M) for 12 h. *G*: densitometric quantification revealed that membrane fluorescence was higher in ANG II-treated cells compared with untreated (CT) cells. Data are means ± SE; $n = 3$. *$P < 0.05$.

G)

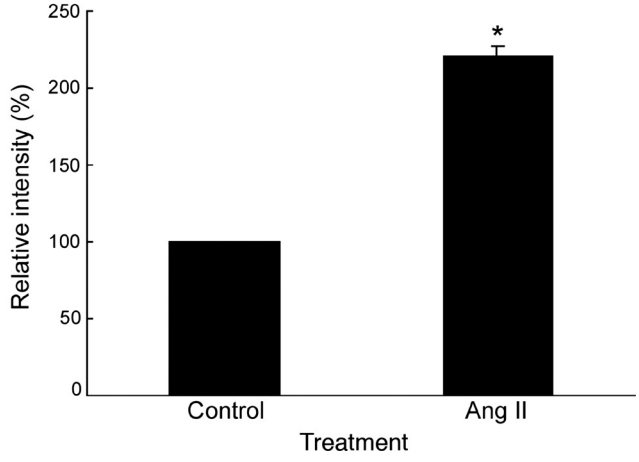

were grown and treated with ANG II or NaCl as described in *Cell culture, reagents, and antibodies*. After treatment, cells were fixed for 20 min at room temperature in 4% paraformaldehyde (Electron Microscopy Sciences, Hatfield, PA), diluted in 0.1 M phosphate buffer, pH 7.4. After three washes in PBS pH 7.4, cells were permeabilized for 3 min with 0.1% Triton X-100 diluted in PBS. Nonspecific staining was blocked by incubating cells with PBS containing 0.5% BSA. Fixed cells were then incubated for 1 h in mouse-anti-zonula occludens-1 antibody diluted 1:10 in PBS (Chemicon, Temecula, CA). An affinity purified polyclonal rabbit anti-serum raised against AQP1 protein purified from human red blood cells and characterized as previously described (54) was subsequently applied at a dilution of 1:100 in PBS for 1 h. After incubation, cells were washed three times with PBS. The cells were then incubated for 1 h with a mixture of both Alexa 488-conjugated goat anti-rabbit IgG (3 μg/ml; Molecular Probes, Eugene, OR) and indocarbocyanine (Cy3) conjugated goat anti-mouse IgG (1.25 μg/ml; Jackson ImmunoResearch, West Grove, PA). Coverslips were then mounted on slides in 1:1 Vectashield:0.3 mM Tris·HCl pH 8.0 (Vector Labs, Burlingame, CA) to retard quenching of the fluorescence signal. Images were acquired using a Nikon Eclipse TE2000-U inverted microscope equipped with a PerkinElmer UltraVIEW spinning disc confocal and a Nikon Plan Apo 60× 1.45 NA objective lens. *Z* slices were captured at 0.1-μm intervals at an exposure time of 1 s. Three-dimensional (3D) reconstructions were made using the Volocity (Improvision, Waltham, MA) software package, and figures were prepared using Adobe Photoshop (Adobe, Newton, MA).

In parallel, a second series of coverslips were treated as described above. After fixation, the cells were stained with only the rabbit anti-AQP1 antibody followed by Cy3-conjugated goat-anti-rabbit IgG antibody (1.5 μg/ml; Jackson ImmunoResearch). Images were taken using a Zeiss Radiance 2000 confocal microscope (Zeiss, Thornwood, NY) with a Zeiss 63× 1.4 NA objective lens. Quantification of AQP1 in cells was performed using IPlab Spectrum software (BD Biosciences) on confocal images. The fluorescence of more than 50 cells from 3 independent experiments was estimated. The mean pixel intensity of the basolateral membrane of cells was quantified, and the background was corrected by the subtraction of the mean pixel intensity of the nucleus. Only cells in the middle of the field of view were quantified to ensure conditions of even illumination. Results were expressed as the amount of fluorescence per unit area, with the control value normalized to 100%.

SDS-PAGE and Western blotting of cell membrane preparations. Cells were cultured in 60-mm Petri dishes and treated as described in *Cell culture, reagents, and antibodies*. After ANG II or NaCl treatment, the confluent cells were washed twice with cold PBS to remove culture medium. Cells were lysed in 150 μl of cold RIPA buffer (Boston Bioproducts, Boston, MA) supplemented with protease inhibitor (Roche Diagnostics). Cell debris was pelleted at 13,000 *g*. The concentration of the solubilized protein from the supernatant was determined using the BCA protein assay (Pierce Biotechnology, Rockford, IL). Membrane preparations were solubilized by heating at 70°C for 10 min in the reducing sample buffer (Invitrogen). Proteins (15 μg) were separated by electrophoresis on NuPAGE 4–12% Bis-Tris gel following the manufacturer's protocol (Invitrogen), following which proteins were electroblotted on polyvinylidene difluoride filters (90 min, 4°C, 100 V; Bio-Rad). Subsequently, the membranes were blocked in blotting buffer PBS Tween 0.1% and 5% nonfat dry milk. Membranes were incubated in the presence of primary antibody, immunopurified rabbit-anti-AQP1 antibody diluted 1:500 in PBS, 0.1% Tween, and 3% nonfat dry milk. After 2 h of incubation and four washes in PBS Tween 0.1% solution, the membrane was incubated for 1 h with 0.5 μg/ml horseradish peroxidase (HRP)-conjugated donkey anti-rabbit antibody (Jackson ImmunoResearch). After four washes, the peroxidase activity was detected with ECL enhanced chemiluminescence system (PerkinElmer, Boston, MA) and Biomax XAR film (PerkinElmer). After exposure, the membrane was acid stripped with 0.2 M glycine-HCl pH 2.5, Tween 0.05% for 1 h and reincubated with mouse anti-actin antibody (0.1 μg/ml Chemicon International, Temecula, CA) and a HRP-conjugated donkey anti-mouse antibody (0.8 μg/ml; Jackson ImmunoResearch) as loading control. The band intensities were quantified from scanned film images using IPlab Spectrum software (BD Biosciences).

Immunocytochemistry on rat kidney sections. Alzet osmotic minipumps (Durect, Cupertino, CA) delivering either a solution of acetic acid 5% (sham) or ANG II diluted in acetic acid 5% solution (80 ng/min) were implanted in rats. A group of ANG II-treated rats received food containing a nonpeptidic ANG II antagonist (olmesartan, 5 mg/day) as described in *Animal treatments* and in a previous study (37). After treatment, animals were euthanized, and then kidneys were harvested, fixed, and embedded in paraffin as previously described (37). Four-micrometer kidney sections mounted on slides were heated for 1 h at 65°C before being deparaffinized in xylene and rehydrated through a series of alcohol baths (100, 75, 50, and 25%). Kidney sections were washed three times in PBS before blocking for 20 min with PBS, BSA 1%. The kidney sections were then incubated for 1 h in the presence of the immunopurified rabbit anti-AQP1 antibody (1:200). Kidney sections were washed three times with PBS before 1 h incubation with Cy3-conjugated goat anti-rabbit IgG antibody. After three washes with PBS, the sections were mounted in 1:1 Vectashield:Tris·HCl 0.1 mM pH 8.0 solution. Immunofluorescence images were taken using a 20 × 0.65 NA objective lens installed on an epifluorescence microscope (Nikon Eclipse E800) equipped with a Hamamatsu Orca CCD camera and using IPLab spectrum software (BD Biosciences). For each kidney section, more than 10 images of the cortex, outer stripe, and papilla were taken. All images were analyzed using IPLab Spectrum software (BD Biosciences). Thus the apical membrane fluorescence of 30–50 tubules from each part of the kidney was studied. The maximal exposure time was set at 100 ms to avoid pixel saturation in the papilla, and each subsequent image was taken with this identical exposure time setting. The mean apical pixel intensity of AQP1 fluorescence is reported as the background-subtracted pixel intensity to the total apical mean pixel intensity.

SDS-PAGE and Western blot analysis of rat kidney membrane preparations. After treatment as described above, rats were anesthetized with isofluorane, and kidneys were harvested. Kidneys were homogenized in cold hypotonic buffer (Tris·HCl pH 7.4, 3 mM $MgCl_2$, and 1 mM EDTA containing complete protease inhibitor cocktail; Roche Applied Science). Homogenized kidney

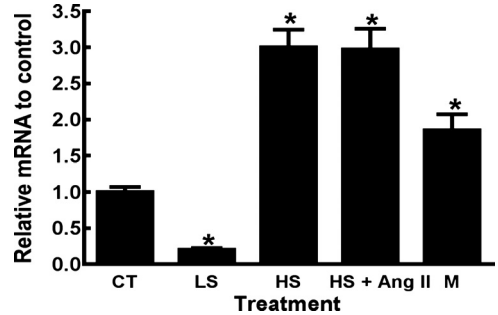

Fig. 4. Real-time PCR indicates that hypertonicity has a biphasic effect on AQP1 mRNA regulation. IRPTC were incubated with various NaCl concentrations: control isotonic (CT =150 mM), low salt (LS = 90 mM), and high salt (HS = 220 mM) for 12 h. AQP1 mRNA expression was also studied in the presence of mannitol (M; 440 mosM/l) as well as high salt plus ANG II (10^{-8}M; HS + ANG II). Relative AQP1 mRNA content measured by real-time RT-PCR was expressed as a function of AQP1 mRNA level under isotonic conditions (CT). AQP1 mRNA expression is significantly decreased in the low-salt condition and significantly increased in the high-salt condition. Both mannitol and HS + ANG II conditions significantly increased AQP1 mRNA vs. control. Data are means ± SE. *$P < 0.001$.

tissue preparations were centrifuged at 100 *g* for 10 min at 4°C. The supernatants were then recentrifuged for 30 min at 35,000 *g* at 4°C. Pellets were resuspended in RIPA buffer containing protease inhibitor cocktail and stored at −80°C. The solubilized protein concentrations were determined using the BCA protein assay, and 35 μg were separated by SDS-PAGE and analyzed by Western blot as described above. Images were taken using a UVP bioimaging system (LLC Upland) instead of Biomax XAR film. After exposure, the membrane was acid stripped with 0.2 M glycine-HCl pH 2.5, Tween 0.05% for 1 h and reincubated with mouse anti-actin antibody (0.1 μg/ml; Chemicon International) and a HRP-conjugated donkey anti-mouse antibody (0.8 μg/ml; Jackson ImmunoResearch) as loading control. The band intensities from digitalized images were quantified using IPlab Spectrum software (BD Biosciences).

Statistics. One-way ANOVA with Bonferroni corrections was performed on the relative intensity values of fluorescence images using StatView. Analytic comparisons of mRNA expression levels were also done using the StatView (Brainpower, Calabasas, CA). Significance levels were set at $P < 0.05$.

RESULTS

ANG II increases AQP1 expression in an AT_1R-dependent manner in IRPTC. After 1 and 6 h of exposure to ANG II, AQP1 mRNA expression was not significantly changed ($P < 0.05$ $n = 4$; data not shown). In contrast, a marked dose-dependent upregulation of expression was detectable after 12 h of exposure to ANG II ($P < 0.001$; $n = 4$; Fig. 1) with a maximum effect at 10^{-8} M ANG II. To determine whether AT_1R or AT_2R was involved in this process, cells were exposed to the selective AT_1R blocker losartan at 10^{-5} M before 10^{-8} M ANG II treatment for 12 h. As shown in Fig. 2, losartan prevented the increase in AQP1 mRNA expression.

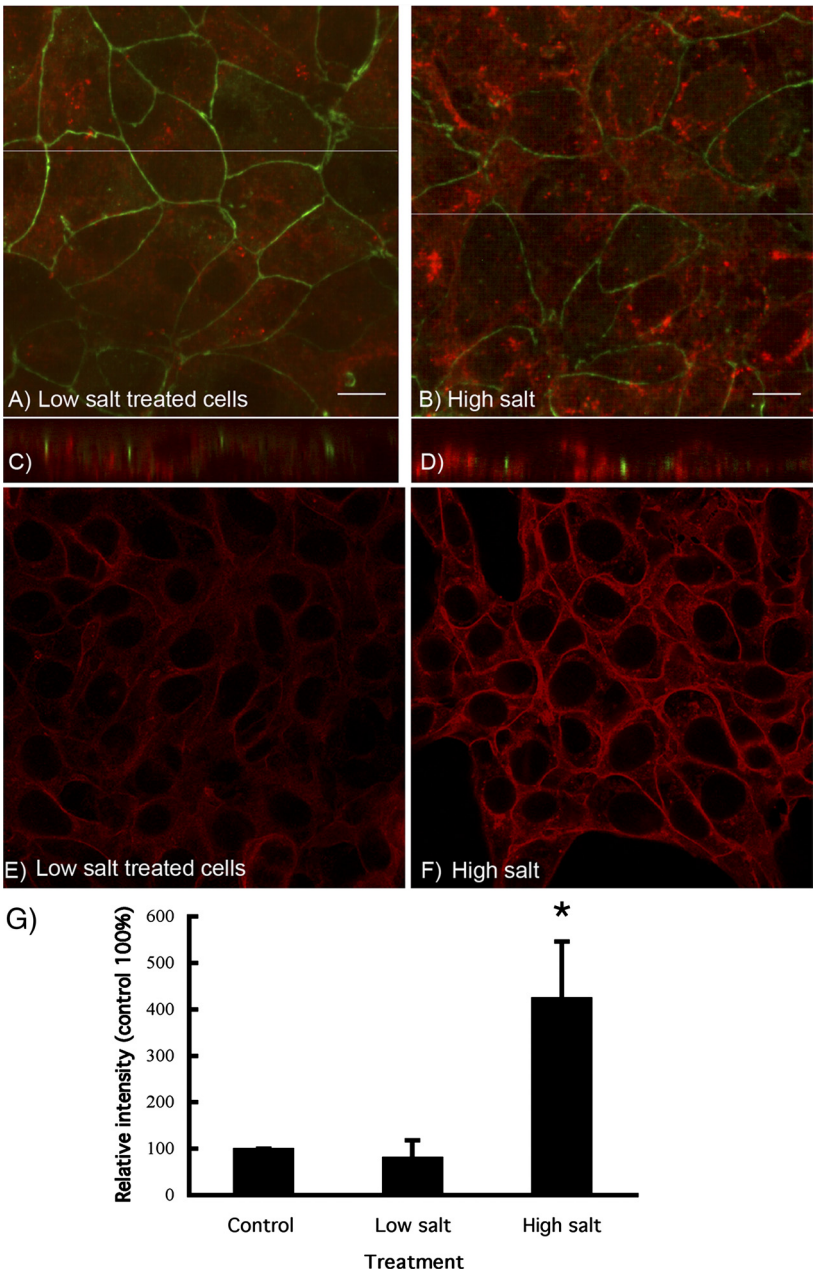

Fig. 5. Confocal microscopy reveals AQP1 staining intensity decreases in low-salt and increases in high-salt conditions. *A–D*: maximum projection and *XZ* slice (taken at the white line) of three-dimensional reconstructions of IRPTC incubated in low salt (90 mM NaCl; *A* and *C*) or high salt (220 mM NaCl; *B* and *D*) for 12 h. The *Z* projections reveal a decrease of AQP1 (red) staining on both apical regions [above the zonula occludens-1 (green) staining] as well as in basolateral membranes in the presence of low salt and an increase in these regions in the presence of high salt. Staining intensity of AQP1 in a single midnuclear confocal plane is illustrated for IRPTC treated with low salt (*E*) or cells treated with high salt (*F*) for 12 h. *G*: densitometric quantification revealed that membrane fluorescence was lower in cells treated with low salt and higher in cells treated with high salt compared with untreated (CT) cells (see also Fig. 3*E*). Data are means ± SE; $n = 3$. *$P < 0.05$.

Addition of the AT_1R antagonist alone significantly decreased AQP1 mRNA ($P < 0.001$; $n = 4$), whereas the selective AT_2R antagonist PD123319 (10 μM) showed no significant effect (data not shown).

The effect of ANG II on AQP1 protein levels was determined using indirect immunofluorescence in IRPTC. Cells treated with ANG II showed an increase in staining intensity compared with untreated cells as assessed by both single plane confocal images as well as 3D reconstruction (Fig. 3, *A* and *E*, respectively). Densitometric analysis of single confocal planes showed a twofold increase in AQP1 membrane fluorescence (Fig. 3*G*). Using zonula occludens-1 (a tight junction marker) staining to delimit apical from basolateral membrane domains in 3D reconstructions (Fig. 3, *C* and *D*), we observed in respective *z*-series images that ANG II increased AQP1 expression in both apical and basolateral poles of the cell (Fig. 3*D*). In the basal state, the AQP1 immunofluorescence appeared primarily in the basolateral plasma membrane. There was also some labeling of cytoplasmic vesicles localized on the subapical cytoplasmic-facing surface of the membrane (Fig. 3*C*). This finding is consistent with previous reports (51, 54) on proximal tubule cells in the intact kidney. In the presence of ANG II, an increase of immunofluorescence staining in the perinuclear cytoplasmic region was also observed (Fig. 3, *B* and *F*). This area is generally associated with the rough endoplasmic reticulum and Golgi and might, therefore, contain newly synthesized AQP1 channels. The increase in AQP1 protein expression is supported by Western blot analysis of the IRPTC treated with ANG II (10^{-8} M), which shows a significant increase of AQP1 expression (see Fig. 6).

Hypertonicity increases AQP1 expression. To assess whether AQP1 is sensitive to alterations of sodium, IRPTC were incubated with various NaCl concentrations: isotonic conditions (150 mM NaCl), low salt (90 mM NaCl), high salt (220 mM NaCl), and mannitol (440 mM). After 12 h in low-salt conditions, AQP1 mRNA was significantly downregulated ($P < 0.001$; $n = 4$). In contrast, AQP1 mRNA was increased twofold under high-salt conditions ($P < 0.001$; $n = 4$; Fig. 4). Hypertonicity modulates AQP1 expression, since mannitol also significantly increased AQP1 mRNA expression twofold compared with control ($P < 0.01$; $n = 4$; Fig. 4). Also, addition of ANG II (10^{-8} M) under high-salt conditions did not further increase AQP1 mRNA expression, suggesting no additive effects of these two stimuli. (Fig. 4; $P < 0.01$). We also assessed AQP1 immunostaining in the cells incubated for 12 h in different NaCl concentrations. Single plane images and 3D reconstruction showed an increase of AQP1 staining (Fig. 5, *F* and *B*, respectively), whereas a decreased staining intensity occurred in cells incubated in low-salt conditions (Fig. 5, *E* and *A*, respectively). Densitometric analysis of single confocal planes showed that AQP1 membrane staining was increased fourfold by high salt ($P < 0.05$; $n = 4$), while it was slightly decreased in low salt (Fig. 5*G*). 3D reconstructions showed an increase of AQP1 staining in both apical and basolateral poles of high-salt-treated cells and a reduction in both poles of AQP1 in low-salt-treated cells (Fig. 5, *D* and *C*, respectively). Western blot analysis in cells treated with high salt and low salt confirmed these findings: an increase of AQP1 expression in hypertonic medium and a diminution of AQP1 expression in hypotonic solution (Fig. 6).

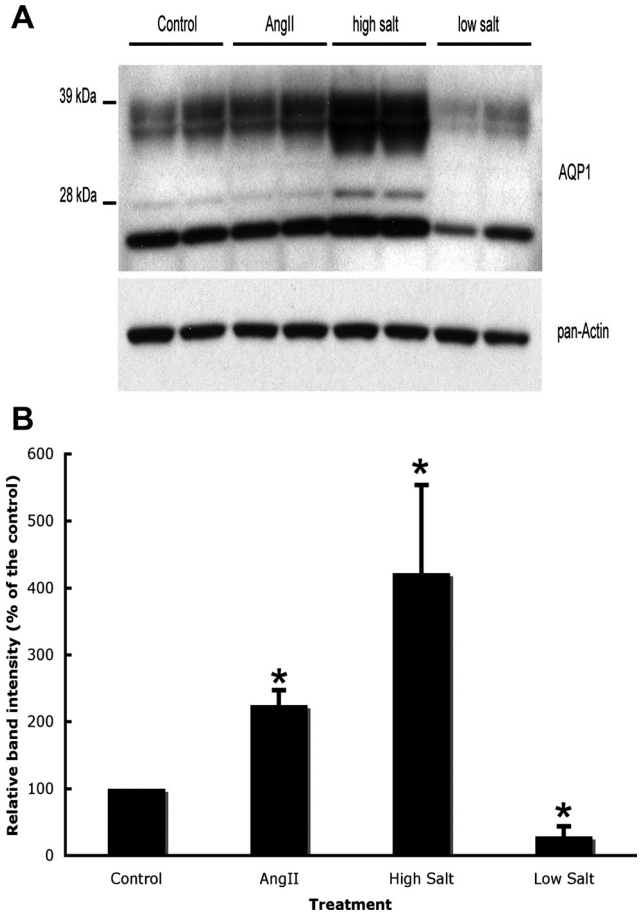

Fig. 6. Western blot analysis shows that ANG II and hypertonicity increase AQP1 expression in IRPTC. *A*: IRPTC were treated for 12 h in isotonic media in the absence (*lanes 1* and *2*) or presence of ANG II (10^{-8}M; *lanes 3* and *4*), as well as in high-salt (220 mM NaCl; *lanes 4* and *5*) or low-salt (90 mM NaCl; *lanes 7* and *8*) conditions. Whole cell homogenates were separated by SDS-PAGE, and AQP1 was detected by Western blot using an anti-AQP1 antibody. Each condition was performed in duplicate. This Western blot analysis represents 3 independent experiments. After exposure, the blots were acid stripped and reincubated with a pan-actin antibody as a protein loading control. *B*: densitometric analysis of the combined intensity of the 28-kDa nonglycosylated AQP1 band and the glycosylated band at 35–45 kDa showed that ANG II and the high-salt condition increase AQP1 expression, while low salt resulted in a reduction of the AQP1 expression. Data are means ± SD; $n = 3$. *$P < 0.05$.

ANG II affects AQP1 expression in an AT_1R-dependent manner in rat kidney tubules. The rats infused with ANG II had a significantly higher blood pressure (161 ± 15 mmHg/kg; $n = 3$) than those infused with solvent alone (sham; 109 ± 11 mmHg/kg; $n = 3$) or rats fed with the ANG II antagonist (103 ± 4 mmHg/kg; $n = 3$; $P < 0.01$, *t*-test). After 10 days, the serum osmolarity of each of the three groups was slightly reduced from 284 ± 5 to 269 ± 3 mmHg/kg.

A significant difference in blood osmolality was found between ANG II-treated rats and controls (272 ± 1 vs. 267 ± 1; $n = 3$; $P < 0.01$). ANG II-treated rats had significantly lower urine osmolarity after 10 days treatment than at *day 0* (1,785 ± 389 vs. 1,613 ± 408 mmHg/kg; $n = 3$; $P < 0.05$), while no significant difference was observed in sham-operated controls (2,025 ± 166 vs. 2,243 ± 78 mmHg/kg; $n = 3$) and antagonist-infused rats (2,209 ± 309 vs. 2,197 ± 125 mmHg/kg; $n = 3$; Fig. 7*A*). The most potent effect of ANG II was observed after the first day of

treatment when urine volume increased by 158% and osmolarity was reduced by 44%. This effect of ANG II on urine osmolarity seems to be attenuated after *day 2*, when the reduction of urine osmolarity was 20% , and it then stabilized around 10% reduction up to the end of the treatment. This effect of ANG II was not seen in the rats treated with ANG II and the ANG II antagonist. Interestingly, urine volume increased a few days after ANG II treatment (Fig. 7*B*), while water intake of the ANG II-treated rats was reduced the first day and increased on the second day (Fig. 7*C*). ANG II-treated rats lost significant weight in the few days of the treatment but then gained it back rapidly thereafter (Fig. 7*D*). These variations in water intake, urine volume, and weight were not observed in untreated rats and rats treated with olmesartan (Fig. 7, *B–D*).

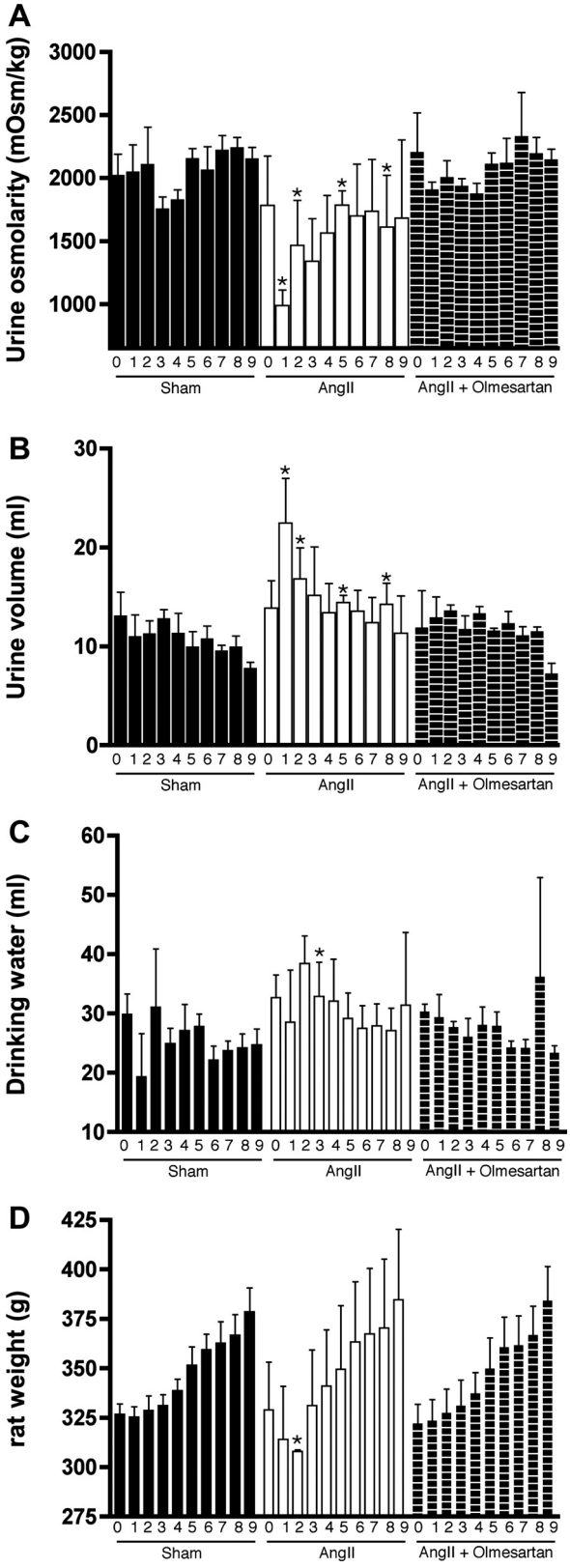

Fig. 7. ANG II affects urine osmolarity, urine volume, and water intake in vivo. Rats with minipumps that deliver either sham solution (closed bar) or 80 ng of ANG II per min (opened and hatched bars) were put into metabolic cages. Some rats were fed with olmesartan (hatched bars), an ANG II antagonist. For 10 days, 24-h urine osmolarity (*A*), urine volume (*B*), water intake volume (*C*), and rat weight (*D*) were measured, and these values were compared with the 24 h metabolic baseline value of rats (*day 0*). Each bar represents an average of 3 rats ± SD ($n = 3$; $^*P < 0.05$, *t*-test).

The effect of rat ANG II infusion on AQP1 kidney expression was examined by immunocytochemistry (Fig. 8). *Insets* show the usual bright AQP1 staining that is normally observed (54) in the cortex (Fig. 8*A*), S3 segment (Fig. 8*E*), and papilla (Fig. 8*I*). For the quantification, we reduced the antibody concentration to reach a linear, nonsaturated range of staining in all sections from rats with and without ANG II treatment. An increase of AQP1 expression in apical and basolateral membranes was observed in the presence of ANG II in the cortex (Fig. 8*B*) and in the papilla (Fig. 8*J*) compared with the control rats (Fig. 8, *A* and *I*, respectively). A small increase in AQP1 fluorescence in apical and basolateral membranes of the S3 segment was also found in the presence of ANG II (Fig. 8*F*) vs. S3 segments from control rats (Fig. 8*E*). This increase of AQP1 expression in ANG II-infused rat kidney was abolished by the selective AT_1R antagonist olmesartan in the cortex (Fig. 8*C*), S3 segment (Fig. 8*G*), and papilla (Fig. 8*K*). Semiquantitative immunocytochemical analysis of sections from ANG II-infused rat kidneys (Fig. 8, *D*, *H*, and *L*) also showed two times more AQP1 in cortical proximal tubules (Fig. 8*D*) and the TDLH (Fig. 8*L*) than in control rats (Fig. 8, *D* and *L*). However, ANG II treatment did not have a significant effect on AQP1 expression in proximal tubule segment 3 (Fig. 8*H*) compared with the control (Fig. 8*H*). This increase of AQP1 expression in ANG II-infused rat kidney was abolished by the selective AT_1R antagonist olmesartan in the cortex (Fig. 8*D*), S3 segment (Fig. 8*H*), and papilla (Fig. 8*L*).

Western blot analysis of whole kidney membrane preparations did not show a significant increase in AQP1 expression in ANG II-treated rat kidneys, and treatment with olmesartan, the ANG II antagonist, showed a marginal reduction of AQP1 expression compared with ANG II-treated rats ($P = 0.053$; Fig. 9).

DISCUSSION

The present study demonstrates that ANG II influences the expression of the water channel AQP1 both in vitro and in vivo. Our data on IRPTC demonstrate that AQP1 mRNA and protein levels can be modulated directly by ANG II via the AT_1R. A role for ANG II on AQP1 expression is also suggested by several previous studies. Wintour et al. (67) demonstrated that exogenous infusion of ANG I into the jugular vein of fetal sheep for 3 days during the last trimester increased

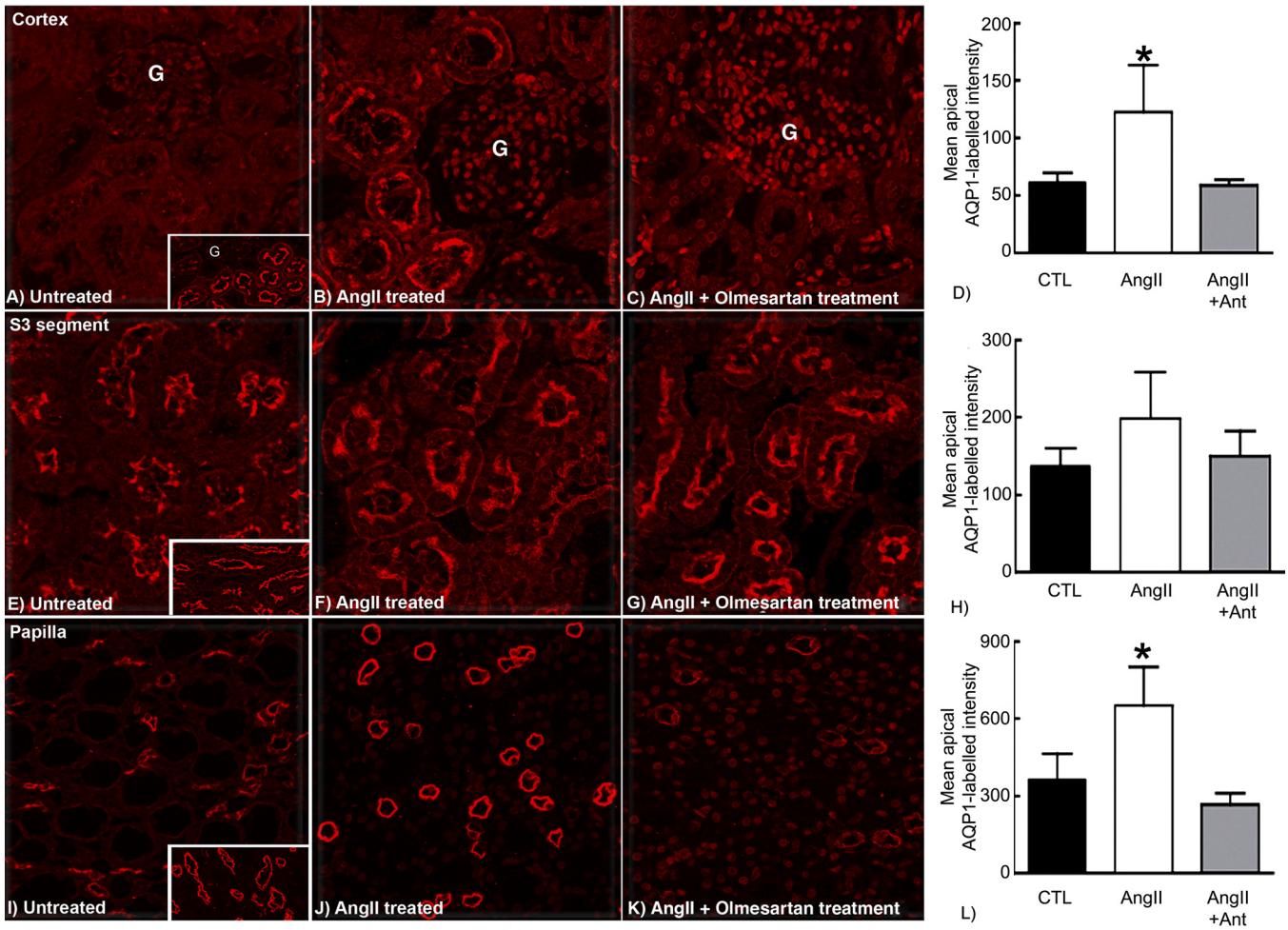

Fig. 8. ANG II increases AQP1 immunofluorescence staining in rat kidneys in vivo, and an AT_1R antagonist inhibits this effect. AQP1 immunostaining was performed on paraffin-embedded rat kidney sections. Sections from normal rats (*A*, *E*, and *I*), ANG II (10^{-8} M)-infused rats (*B*, *F*, and *J*), and ANG II (10^{-8} M)- and olmesartan (10^{-5} M)-infused rats (*C*, *G*, and *K*) were incubated with a low concentration of anti-AQP1 antibody. All images were acquired using identical exposure times. AQP1 expression in cortex (*A–C*), S3 proximal tubule segments (PTs; *E–G*), and papilla (*I–K*) was compared, and a densitometric analysis showed an increase of AQP1 staining in proximal tubule segments 1 and 2 (*D*) and in thin descending limb of Henle (*L*) but not in the PT S3 segment (*H*). Note that to obtain a linear, nonsaturated range of staining in all sections from rats with and without ANG II treatment, the antibody concentrations used to generate these figures was reduced so that PTs from normal control rats were stained more weakly than is normally observed (54). Examples of the usual bright AQP1 staining in PTs of normal rats using an optimal antibody concentration and exposure times are illustrated for comparison in *insets* of *A*, *E*, and *I*. AQP1 staining is more abundant in PTs (*B*) and in thin descending limb of Henle (*J*) in animals treated with ANG II compared with rats not treated with the octapeptide (*A* and *I*, respectively). The pattern of AQP1 staining in kidneys of animals infused with ANG II plus olmesartan is similar to that in untreated rats. Images of rat kidney sections are representative of images obtained with animals treated under similar conditions (6 per group). Fluorescence intensity of 20 cells from each kidney sections were quantified. Data are means ± SD; $n = 6$. *$P < 0.05$, one-way ANOVA (G: glomerulus in *A* and *insets*).

intrarenal AQP1 mRNA expression in the fetal kidney, presumably via conversion of the infused ANG I to ANG II. In other studies, Klein et al. (34) demonstrated impaired urinary concentration associated with reduced intrarenal AQP1 expression in mice lacking ACE. While several other studies (17, 27, 34, 38, 63) employing ACE inhibitors and selective AT_1R antagonists suggested a role for ANG II in AQP1 expression, they did not provide direct evidence for such an action of ANG II. Our present data now show that ANG II directly affects AQP1 expression in vitro and, importantly, show that ANG II infusion also regulated AQP1 membrane expression in proximal tubules in vivo. These observations are consistent with a large body of evidence indicating that ANG II is involved in H^+, sodium, bicarbonate, and water transport in the proximal tubule (8, 21, 43, 48, 55, 58).

In addition, the effects of ANG II on water and salt reabsorption by the proximal tubule are both dose dependent and biphasic; low concentrations (10^{-12} to 10^{-8} M) stimulate sodium and water reabsorption, whereas high doses of ANG II (10^{-7} to 10^{-5} M) appear to have inhibitory effects (4, 8, 10, 20, 42, 58). In the present studies, 10^{-8} M ANG II increased both AQP1 mRNA and protein levels after 12 h of exposure. The increases in AQP1 mRNA induced by ANG II were inhibited by losartan, implicating the AT_1R as the mediator of the response, which is also consistent with actions on sodium and bicarbonate transport.

The AQP1 protein was detected in IRPTC by Western blotting and immunostaining. Immunofluorescence results indicate that the AQP1 protein is inserted into the plasma membrane without significant accumulation in an intracellular

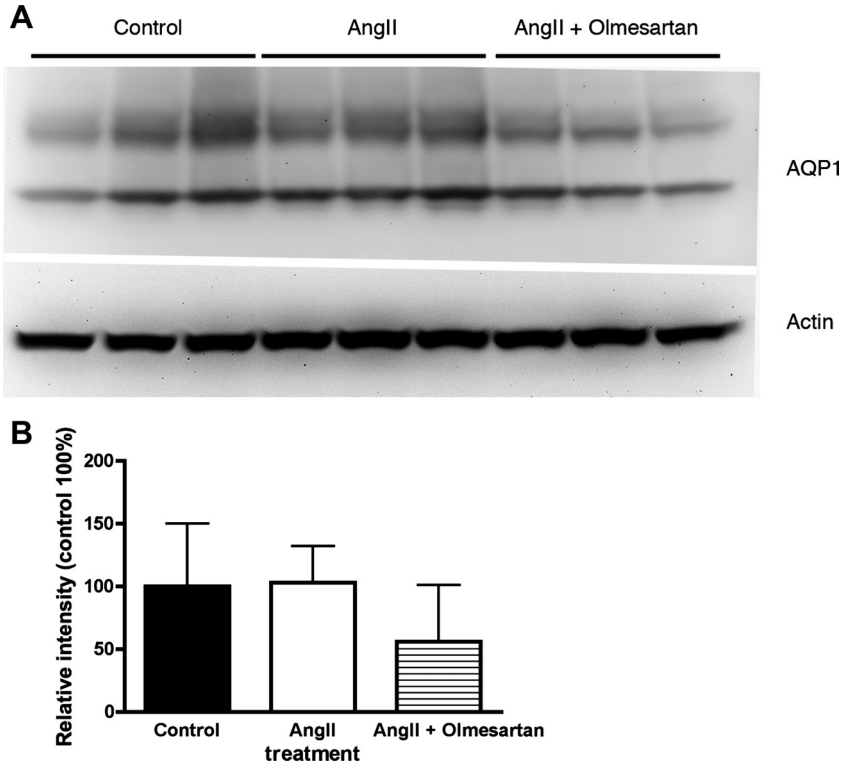

Fig. 9. *A*: Western blot analysis of AQP1 expression in control and ANG II-treated rat kidney. Rats were treated 10 days with minipumps delivering vehicle alone (control) or 80 ng of ANG II per min. Membrane kidney homogenates were separated by SDS-PAGE, and AQP1 was detected by Western blot using an anti-AQP1 antibody. Each condition was performed in 3 rats. After exposure, the blot was acid-stripped and reincubated with a pan-actin antibody as a protein loading control. *B*: densitometric analysis of the combined intensity of the 28-kDa nonglycosylated AQP1 band and the glycosylated band at 35–45 kDa showed that ANG II slightly increased AQP1 expression while olmesartan resulted in a reduction of AQP1 expression. Data are means ± SD; $n = 3$.

compartment. The levels of membrane-associated AQP1 detected by immunocytochemistry and Western blot increased 12 h after ANG II (10^{-8} M) stimulation. However, aside from intensity levels, no qualitative difference in the staining pattern between stimulated and control cells could be detected, and no evidence of a regulated shuttle mechanism for the membrane insertion of AQP1, such as that seen for the collecting duct water channel AQP2, was detectable (14, 18, 33, 50, 53). Signaling pathways for ANG II within the proximal tubule are complex and numerous, and the specific mechanism by which ANG II affects AQP1 expression is currently not known. Torres et al. (64) showed in 1978 that ANG II inhibits adenylyl cyclase within the proximal tubule. Since then, several studies (28, 43) have suggested that ANG II stimulates sodium transport by inhibiting adenylyl cyclase. However, several cAMP-independent pathways have also been reported, such as activation of phospholipase A_2 (15) and activation of phospholipase C (8). cAMP upregulates expression of AQP2, and cAMP-responsive elements have been detected in the 5′-flanking region of the AQP2 gene (26). Using a *Xenopus* oocyte expression system, Yool et al. (70) showed regulation of AQP1 permeability via a cAMP-dependent mechanism. In their experiments, forskolin induced a cation current in AQP1-expressing oocytes. However, other laboratories (2, 13, 66) could not reproduce those results. However, other work published by Anthony and collegues reported that AQP1 not only mediates water flux but also serves as a cGMP-gated ion channel (3) or CO_2 transport (11, 16).

The present studies, using an in vitro system of immortalized rat proximal tubular cells, demonstrate that AQP1 mRNA and protein are upregulated by extracellular hypertonicity for 12 h, possibly via transcriptional activation or posttranscriptional regulation such as increased mRNA stability. Hypertonicity-induced AQP1 expression involves the MAPK pathway and the hypertonicity-responsive element (65). Previous studies have clearly shown that AQP2 expression and trafficking are also regulated by tonicity (6, 24, 25, 60) and that increased membrane accumulation of AQP2 in response to hypertonicity is MAPK dependent (25). However, Leitch et al. (40) showed that the increase in AQP1 protein expression induced by hypertonic stress was due to reduced protein ubiquitination and increased protein stability. Abrami et al. (1) demonstrated that salt acclimation increased expression of the water channel FA-CHIP-mRNA, an aquaporin of the frog urinary bladder, using the model of toad skin and urinary bladder. Similar observations followed using epithelial cell cultures (29, 30). In our studies, addition of ANG II (10^{-8} M) to cells incubated in high-salt conditions (220 mM) did not further increase AQP1 mRNA expression.

The concentration of salt in the interstitial fluid varies along the renal cortico-medullary axis. This gradient is necessary for the urinary concentrating mechanism to function but also has significant effects on the responsiveness of cells to an antidiuretic hormone (71). Cells in the inner medulla are exposed to variable and high levels of NaCl and undergo adaptive responses (7, 49). Most cells are normally not stressed by hypertonicity, because the concentration of NaCl is closely controlled in all extracellular body fluid compartments, the kidney medulla being a remarkable exception. This implies that ANG II rather than osmolality is likely to be more important in regulating AQP1 levels in the proximal tubule. In the present study, AQP1 mRNA is downregulated in IRPTC in response to low salt; this mechanism might play an important role in chronic intracellular volume regulatory mechanisms. Proximal renal tubule cells may adjust intracellular volume in hypotonic extracellular media owing not only to loss of solute but also through chronic modulation of AQP1. Whether a

similar mechanism occurs in the cells of the TDLH remains to be determined, but this segment is certainly exposed to variations in extracellular osmolality to a greater extent than are cells of the proximal convoluted tubule in the cortex.

Our in vivo study showed that in the kidney, ANG II is an important agent in volume-mediated fluid expansion, which regulates long-term arterial pressure as proposed by Guyton (19), who suggested that dysregulation of body fluid volume is a requisite for the pathogenesis of hypertension. The ANG II-infused rats have high blood pressure, higher urinary volume, decreased urinary osmolarity, increased fluid intake and significant weight gain due to volume expansion, suggesting increased sodium and water reabsorption. Whole kidney AQP1 expression was not measureably increased in the ANG II-infused animals but was significantly decreased by AT_1R antagonist (olmesartan) treatment. Although total kidney AQP1 was not increased, we quantified a twofold increase of AQP1 fluorescence intensity in the proximal tubule and TDLH in the ANG II-infused rats, suggesting a redistribution of AQP1 expression that affected the staining intensity, perhaps reflecting an increase in membrane localization similar to our finding in cultured cells. This twofold increase in proximal tubule and TDLH fluorescence intensity was abolished by the AT_1R antagonist (olmesartan). We suggest that ANG II increases AQP1 expression in vitro and in vivo via AT_1R. Nevertheless, the effect of ANG II on TDLH may be indirect because we are assuming that TDLH cells also express the AT_1R. It is possible that AT_1R in TDLH may be expressed at a level that was not detectable in prior studies. However, ANG II treatment has little if any effect on AQP1 expression in the S3 segment where AT_1R is known to be expressed (46). It is possible that the constant presence of ANG II led to a partial desensitization of AT_1R, while such an effect of ANG II was not observed in other tubule areas with lower AT_1R abundance, such as the S1 segment or TDLH (9). Nevertheless, our findings support a critical renal role of ANG II in volume expansion and volume hypertension mediated by the AT_1R. Similar results showing the key roles of RAS mediated by AT_1R in the kidney in volume regulation were demonstrated by Crowley et al. (12) using kidney AT_1R vs. systemic knockout models.

In summary, our data demonstrate that AQP1 mRNA and protein levels in proximal tubule cells can be regulated in vitro by NaCl and ANG II. Due to the relatively stable isotonic environment in the renal cortex, the regulation of AQP1 in this segment is unlikely through hypertonicity. Our results showing that AQP1 is upregulated in proximal cells in culture (IRPTC) and in PT cells in vivo by ANG II, and that this effect is mediated by AT_1R, provide strong evidence in favor of a physiological role for the RAS in this process. In contrast, regulation of AQP1 expression in the medulla (cells of the TDLH) could occur mainly as a response to interstitial NaCl concentration, although a role for ANG II in this tubule segment is also possible.

ACKNOWLEDGMENTS

We thank Dr. Dulce Casarine, Diciplina de Nefrologia UNIFESP/Sao Paulo, Brazil, for allowing us to complete this study in her laboratory during the aftermath of Hurricane Katrina. We also thank Daiichi Sankyo for providing Olmesartan.

GRANTS

These studies were supported by National Heart, Lung, and Blood Institute Grants HL-40210 and HL-48455 (to J. Ingelfinger) and by National Institute of Diabetes and Digestive and Kidney Diseases Grant PO1-DK-38452 (to D. Brown). R. Bouley received the National Kidney Foundation Investigator Award. P. Nunes is supported by a Doctoral Level Postgraduate Scholarship from National Sciences and Engineering Research Council and by National Institute of Diabetes and Digestive and Kidney Diseases Grant DK-38452. The Microscopy Core Facility of the Massachusetts General Hospital Program in Membrane Biology receives additional support from the Boston Area Diabetes and Endocrinology Research Center (DK-57521) and the Center for the Study of Inflammatory Bowel Disease (DK-43351).

DISCLOSURES

No conflicts of interest are declared by the author(s).

REFERENCES

1. **Abrami L, Capurro C, Ibarra C, Parisi M, Buhler JM, Ripoche P.** Distribution of mRNA encoding the FA-CHIP water channel in amphibian tissues: effects of salt adaptation. *J Membr Biol* 143: 199–205, 1995.
2. **Agre P, Lee MD, Devidas S, Guggino WB.** Aquaporins and ion conductance. *Science* 275: 1490; author reply 1492, 1997.
3. **Anthony TL, Brooks HL, Boassa D, Leonov S, Yanochko GM, Regan JW, Yool AJ.** Cloned human aquaporin-1 is a cyclic GMP-gated ion channel. *Mol Pharmacol* 57: 576–588, 2000.
4. **Aperia A, Holtback U, Syren ML, Svensson LB, Fryckstedt J, Greengard P.** Activation/deactivation of renal Na+,K(+)-ATPase: a final common pathway for regulation of natriuresis. *FASEB J* 8: 436–439, 1994.
5. **Blantz RC.** The glomerular and tubular actions of angiotensin II. *Am J Kidney Dis* 10: 2–6, 1987.
6. **Bouley R, Hasler U, Lu HA, Nunes P, Brown D.** Bypassing vasopressin receptor signaling pathways in nephrogenic diabetes insipidus. *Semin Nephrol* 28: 266–278, 2008.
7. **Burg MB, Ferraris JD.** Intracellular organic osmolytes: function and regulation. *J Biol Chem* 283: 7309–7313, 2008.
8. **Chatsudthipong V, Chan YL.** Inhibitory effect of angiotensin II on renal tubular transport. *Am J Physiol Renal Fluid Electrolyte Physiol* 260: F340–F346, 1991.
9. **Cheng HF, Becker BN, Burns KD, Harris RC.** Angiotensin II upregulates type-1 angiotensin II receptors in renal proximal tubule. *J Clin Invest* 95: 2012–2019, 1995.
10. **Cogan MG.** Angiotensin II: a powerful controller of sodium transport in the early proximal tubule. *Hypertension* 15: 451–458, 1990.
11. **Cooper GJ, Zhou Y, Bouyer P, Grichtchenko II, Boron WF.** Transport of volatile solutes through AQP1. *J Physiol* 542: 17–29, 2002.
12. **Crowley SD, Gurley SB, Herrera MJ, Ruiz P, Griffiths R, Kumar AP, Kim HS, Smithies O, Le TH, Coffman TM.** Angiotensin II causes hypertension and cardiac hypertrophy through its receptors in the kidney. *Proc Natl Acad Sci USA* 103: 17985–17990, 2006.
13. **Deen PM, Mulders SM, Kansen SM, van Os CH.** Aquaporins and ion conductance. *Science* 275: 1491; author reply 1492, 1997.
14. **Deen PM, Verdijk MA, Knoers NV, Wieringa B, Monnens LA, van Os CH, van Oost BA.** Requirement of human renal water channel aquaporin-2 for vasopressin-dependent concentration of urine. *Science* 264: 92–95, 1994.
15. **DiGiovanni SR, Nielsen S, Christensen EI, Knepper MA.** Regulation of collecting duct water channel expression by vasopressin in Brattleboro rat. *Proc Natl Acad Sci USA* 91: 8984–8988, 1994.
16. **Endeward V, Musa-Aziz R, Cooper GJ, Chen LM, Pelletier MF, Virkki LV, Supuran CT, King LS, Boron WF, Gros G.** Evidence that aquaporin 1 is a major pathway for CO_2 transport across the human erythrocyte membrane. *FASEB J* 20: 1974–1981, 2006.
17. **Eskild-Jensen A, Thomsen K, Rungo C, Ferreira LS, Paulsen LF, Rawashdeh YF, Nyengaard JR, Nielsen S, Djurhuus JC, Frokiaer J.** Glomerular and tubular function during AT1 receptor blockade in pigs with neonatal induced partial ureteropelvic obstruction. *Am J Physiol Renal Physiol* 292: F921–F929, 2007.
18. **Fushimi K, Uchida S, Hara Y, Hirata Y, Marumo F, Sasaki S.** Cloning and expression of apical membrane water channel of rat kidney collecting tubule. *Nature* 361: 549–552, 1993.
19. **Guyton AC.** Blood pressure control–special role of the kidneys and body fluids. *Science* 252: 1813–1816, 1991.
20. **Hall JE.** Control of sodium excretion by angiotensin II: intrarenal mechanisms and blood pressure regulation. *Am J Physiol Regul Integr Comp Physiol* 250: R960–R972, 1986.

21. **Harris PJ, Thomas D, Zhuo J, Skinner SL.** Regulation of proximal tubule sodium reabsorption by angiotensin II (AII) and atrial natriuretic factor (ANF). *Acta Physiol Scand Suppl* 591: 63–65, 1990.
22. **Harris PJ, Young JA.** Dose-dependent stimulation and inhibition of proximal tubular sodium reabsorption by angiotensin II in the rat kidney. *Pflügers Arch* 367: 295–297, 1977.
23. **Hasegawa H, Zhang R, Dohrman A, Verkman AS.** Tissue-specific expression of mRNA encoding rat kidney water channel CHIP28k by in situ hybridization. *Am J Physiol Cell Physiol* 264: C237–C245, 1993.
24. **Hasler U, Leroy V, Jeon US, Bouley R, Dimitrov M, Kim JA, Brown D, Kwon HM, Martin PY, Feraille E.** NF-kappaB Modulates aquaporin-2 transcription in renal collecting duct principal cells. *J Biol Chem* 283: 28095–28105, 2008.
25. **Hasler U, Nunes P, Bouley R, Lu HA, Matsuzaki T, Brown D.** Acute hypertonicity alters aquaporin-2 trafficking and induces a MAPK-dependent accumulation at the plasma membrane of renal epithelial cells. *J Biol Chem* 283: 26643–26661, 2008.
26. **Hozawa S, Holtzman EJ, Ausiello DA.** cAMP motifs regulating transcription in the aquaporin 2 gene. *Am J Physiol Cell Physiol* 270: C1695–C1702, 1996.
27. **Imai H, Nakamoto H, Ishida Y, Yamanouchi Y, Inoue T, Okada H, Suzuki H.** Renin-angiotensin system plays an important role in the regulation of water transport in the peritoneum. *Adv Perit Dial* 17: 20–24, 2001.
28. **Jacobson HR.** Altered permeability in the proximal tubule response to cyclic AMP. *Am J Physiol Renal Fluid Electrolyte Physiol* 236: F71–F79, 1979.
29. **Jenq W, Cooper DR, Bittle P, Ramirez G.** Aquaporin-1 expression in proximal tubule epithelial cells of human kidney is regulated by hyperosmolarity and contrast agents. *Biochem Biophys Res Commun* 256: 240–248, 1999.
30. **Jenq W, Mathieson IM, Ihara W, Ramirez G.** Aquaporin-1: an osmoinducible water channel in cultured mIMCD-3 cells. *Biochem Biophys Res Commun* 245: 804–809, 1998.
31. **Jenq W, Ramirez G, Peguero A, Cooper DR, Vesely DL.** D-glucose and NaCl enhance the expression of aquaporin-1: inhibition of both by cholera toxin. *Nephron* 92: 279–286, 2002.
32. **Kastner PR, Hall JE, Guyton AC.** Control of glomerular filtration rate: role of intrarenally formed angiotensin II. *Am J Physiol Renal Fluid Electrolyte Physiol* 246: F897–F906, 1984.
33. **Katsura T, Gustafson CE, Ausiello DA, Brown D.** Protein kinase A phosphorylation is involved in regulated exocytosis of aquaporin-2 in transfected LLC-PK1 cells. *Am J Physiol Renal Physiol* 272: F817–F822, 1997.
34. **Klein JD, Le Quach D, Cole JM, Disher K, Mongiu AK, Wang X, Bernstein KE, Sands JM.** Impaired urine concentration and absence of tissue ACE: involvement of medullary transport proteins. *Am J Physiol Renal Physiol* 283: F517–F524, 2002.
35. **Klein JD, Murrell BP, Tucker S, Kim YH, Sands JM.** Urea transporter UT-A1 and aquaporin-2 proteins decrease in response to angiotensin II or norepinephrine-induced acute hypertension. *Am J Physiol Renal Physiol* 291: F952–F959, 2006.
36. **Knepper MA, Rector PC Jr.** Urinary concentration and dilution In: *Kidney*, edited by Brenner BM, Rector FC. Philadelphia, PA: WB Saunders, 1991, p. 445–482.
37. **Kobori H, Prieto-Carrasquero MC, Ozawa Y, Navar LG.** AT1 receptor mediated augmentation of intrarenal angiotensinogen in angiotensin II-dependent hypertension. *Hypertension* 43: 1126–1132, 2004.
38. **Kwon TH, Nielsen J, Knepper MA, Frokiaer J, Nielsen S.** Angiotensin II AT_1 receptor blockade decreases vasopressin-induced water reabsorption and AQP2 levels in NaCl-restricted rats. *Am J Physiol Renal Physiol* 288: F673–F684, 2005.
39. **Lee YJ, Song IK, Jang KJ, Nielsen J, Frokiaer J, Nielsen S, Kwon TH.** Increased AQP2 targeting in primary cultured IMCD cells in response to angiotensin II through AT_1 receptor. *Am J Physiol Renal Physiol* 292: F340–F350, 2007.
40. **Leitch V, Agre P, King LS.** Altered ubiquitination and stability of aquaporin-1 in hypertonic stress. *Proc Natl Acad Sci USA* 98: 2894–2898, 2001.
41. **Levens NR, Peach MJ, Carey RM.** Role of the intrarenal renin-angiotensin system in the control of renal function. *Circ Res* 48: 157–167, 1981.
42. **Li L, Wang YP, Capparelli AW, Jo OD, Yanagawa N.** Effect of luminal angiotensin II on proximal tubule fluid transport: role of apical phospholipase A2. *Am J Physiol Renal Fluid Electrolyte Physiol* 266: F202–F209, 1994.
43. **Liu FY, Cogan MG.** Angiotensin II stimulates early proximal bicarbonate absorption in the rat by decreasing cyclic adenosine monophosphate. *J Clin Invest* 84: 83–91, 1989.
44. **Livak KJ, Schmittgen TD.** Analysis of relative gene expression data using real-time quantitative PCR and the 2[-delta delta C(T)] method. *Methods* 25: 402–408, 2001.
45. **Llorens-Cortes C, Greenberg B, Huang H, Corvol P.** Tissular expression and regulation of type 1 angiotensin II receptor subtypes by quantitative reverse transcriptase-polymerase chain reaction analysis. *Hypertension* 24: 538–548, 1994.
46. **Meister B, Lippoldt A, Bunnemann B, Inagami T, Ganten D, Fuxe K.** Cellular expression of angiotensin type-1 receptor mRNA in the kidney. *Kidney Int* 44: 331–336, 1993.
47. **Miyata N, Park F, Li XF, Cowley AW Jr.** Distribution of angiotensin AT1 and AT2 receptor subtypes in the rat kidney. *Am J Physiol Renal Physiol* 277: F437–F446, 1999.
48. **Nagami GT.** Effect of angiotensin II on ammonia production and secretion by mouse proximal tubules perfused in vitro. *J Clin Invest* 89: 925–931, 1992.
49. **Neuhofer W, Beck FX.** Survival in hostile environments: strategies of renal medullary cells. *Physiology (Bethesda)* 21: 171–180, 2006.
50. **Nielsen S, DiGiovanni SR, Christensen EI, Knepper MA, Harris HW.** Cellular and subcellular immunolocalization of vasopressin-regulated water channel in rat kidney. *Proc Natl Acad Sci USA* 90: 11663–11667, 1993.
51. **Nielsen S, Smith BL, Christensen EI, Knepper MA, Agre P.** CHIP28 water channels are localized in constitutively water-permeable segments of the nephron. *J Cell Biol* 120: 371–383, 1993.
52. **Pallone TL, Edwards A, Ma T, Silldorff EP, Verkman AS.** Requirement of aquaporin-1 for NaCl-driven water transport across descending vasa recta. *J Clin Invest* 105: 215–222, 2000.
53. **Sabolic I, Katsura T, Verbavatz JM, Brown D.** The AQP2 water channel: effect of vasopressin treatment, microtubule disruption, and distribution in neonatal rats. *J Membr Biol* 143: 165–175, 1995.
54. **Sabolic I, Valenti G, Verbavatz JM, Van Hoek AN, Verkman AS, Ausiello DA, Brown D.** Localization of the CHIP28 water channel in rat kidney. *Am J Physiol Cell Physiol* 263: C1225–C1233, 1992.
55. **Saccomani G, Mitchell KD, Navar LG.** Angiotensin II stimulation of Na(+)-H+ exchange in proximal tubule cells. *Am J Physiol Renal Fluid Electrolyte Physiol* 258: F1188–F1195, 1990.
56. **Schnermann J, Briggs J.** Role of the renin-angiotensin system in tubuloglomerular feedback. *Fed Proc* 45: 1426–1430, 1986.
57. **Schnermann J, Chou CL, Ma T, Traynor T, Knepper MA, Verkman AS.** Defective proximal tubular fluid reabsorption in transgenic aquaporin-1 null mice. *Proc Natl Acad Sci USA* 95: 9660–9664, 1998.
58. **Schuster VL.** Effects of angiotensin on proximal tubular reabsorption. *Fed Proc* 45: 1444–1447, 1986.
59. **Seikaly MG, Arant BS Jr, Seney FD Jr.** Endogenous angiotensin concentrations in specific intrarenal fluid compartments of the rat. *J Clin Invest* 86: 1352–1357, 1990.
60. **Tamma G, Procino G, Strafino A, Bononi E, Meyer G, Paulmichl M, Formoso V, Svelto M, Valenti G.** Hypotonicity induces aquaporin-2 internalization and cytosol-to-membrane translocation of ICln in renal cells. *Endocrinology* 148: 1118–1130, 2007.
61. **Tang SS, Jung F, Diamant D, Brown D, Bachinsky D, Hellman P, Ingelfinger JR.** Temperature-sensitive SV40 immortalized rat proximal tubule cell line has functional renin-angiotensin system. *Am J Physiol Renal Fluid Electrolyte Physiol* 268: F435–F446, 1995.
62. **Tang SS, Jung F, Diamant D, Ingelfinger J.** Immortalized rat proximal tubule cell lines expressing components of the renin-angiotensin system. *Exp Nephrol* 2: 127, 1994.
63. **Topcu SO, Pedersen M, Norregaard R, Wang G, Knepper M, Djurhuus JC, Nielsen S, Jorgensen TM, Frokiaer J.** Candesartan prevents long-term impairment of renal function in response to neonatal partial unilateral ureteral obstruction. *Am J Physiol Renal Physiol* 292: F736–F748, 2007.
64. **Torres VE, Northrup TE, Edwards RM, Shah SV, Dousa TP.** Modulation of cyclic nucleotides in islated rat glomeruli: role of histamine, carbamylcholine, parathyroid hormone, and angiotensin-II. *J Clin Invest* 62: 1334–1343, 1978.
65. **Umenishi F, Schrier RW.** Hypertonicity-induced aquaporin-1 (AQP1) expression is mediated by the activation of MAPK pathways and hypertonicity-responsive element in the AQP1 gene. *J Biol Chem* 278: 15765–15770, 2003.
66. **Verkman AS, Yang B.** Aquaporins and ion conductance. *Science* 275: 1491; author reply 1492, 1997.
67. **Wintour EM, Earnest L, Alcorn D, Butkus A, Shandley L, Jeyaseelan K.** Ovine AQP1: cDNA cloning, ontogeny, and control of renal gene expression. *Pediatr Nephrol* 12: 545–553, 1998.

68. **Wong NL, Tsui JK.** Angiotensin II upregulates the expression of vasopressin V2 mRNA in the inner medullary collecting duct of the rat. *Metabolism* 52: 290–295, 2003.
69. **Yang B, Ma T, Dong JY, Verkman AS.** Partial correction of the urinary concentrating defect in aquaporin-1 null mice by adenovirus-mediated gene delivery. *Hum Gene Ther* 11: 567–575, 2000.
70. **Yool AJ, Stamer WD, Regan JW.** Forskolin stimulation of water and cation permeability in aquaporin 1 water channels. *Science* 273: 1216–1218, 1996.
71. **Zalyapin EA, Bouley R, Hasler U, Vilardaga JP, Lin HY, Brown D, Ausiello DA.** Effects of the renal medullary pH and ionic environment on vasopressin binding and signaling. *Kidney Int* 74: 1557–1567, 2008.